

Impact of a projected future Arctic Sea Ice reduction on extratropical storminess and the NAO

Ivar A. Seierstad · Jürgen Bader

Received: 20 May 2008 / Accepted: 18 August 2008 / Published online: 9 September 2008
© Springer-Verlag 2008

Abstract The impact of a reduced Arctic sea ice cover on wintertime extratropical storminess is investigated by conducting atmospheric general circulation model (AGCM) experiments. The AGCM ECHAM5 is forced by the present and a projected future seasonal cycle of Arctic sea ice. In the experiment with projected sea-ice concentrations significant reductions in storminess were found during December and January in both midlatitudes and towards the Arctic. However, a substantially larger reduction in extratropical storminess was found in March, despite a smaller change in surface energy fluxes in March than in the other winter months. The projected decrease in storminess is also related to the negative phase of the North Atlantic Oscillation (NAO). The March response is consistent with a forcing from transient and quasi-stationary eddies associated with negative NAO events. The greater sensitivity to sea-ice anomalies in late winter sets this study apart from earlier ones.

Keywords Sea-ice · NAO · Storminess · Climate change · Seasonality · AGCM

1 Introduction

Extratropical storms play a dominant role for the midlatitude climate through transports of heat, moisture and

momentum. It is therefore vital in a climate change context to investigate the external factors determining the climatological position and strength of storms. The influence of a declining Arctic sea-ice cover is examined here.

Many IPCC AR4 simulations project a substantial reduction in Arctic sea-ice cover at the end of the twenty-first century (Zhang and Walsh 2006). There are even indications that sea ice is currently declining faster than predicted by most climate models (Eisenman et al. 2007; Stroeve et al. 2007). To investigate the atmospheric response to a projected Arctic sea-ice decline is therefore highly relevant, even though the timing of such reductions remains an open question.

Compared to the vast amount of literature on the atmospheric response to changes in midlatitude SSTs there are relatively few on the response to sea-ice anomalies. However, the removal of sea-ice during winter affects the surface energy fluxes much more than a few degrees increase in SST over already open water (Deser et al. 2004). Magnusdottir et al. (2004) found in a modelling study that idealized negative sea-ice anomalies in the Greenland Sea induced a negative response in the North Atlantic Oscillation (NAO) with weaker and southward shifted storm tracks in the winter season. Alexander et al. (2004) reached a similar conclusion from modelling of more realistic sea-ice anomalies during DJF. Furthermore, Kvamstø et al. (2004) emphasised the role of sea-ice anomalies in the Labrador Sea for forcing a negative NAO response in JFM. The common theme is thus that Arctic sea-ice reductions induce a negative “NAO-like” response during winter, albeit a fairly weak one. More recently, Singarayer et al. (2006) forced the Hadley Centre Atmospheric model with observed 1980–2000 sea-ice extent and with projected sea-ice reductions through 2100. They did not find a negative NAO response. In fact one of their runs even showed an intensified North Atlantic storm track.

I. A. Seierstad
Geophysical Institute, University of Bergen,
Allégaten 70, 5007 Bergen, Norway
e-mail: ivar.seierstad@gi.uib.no

J. Bader (✉)
Bjerknes Centre for Climate Research,
Allégaten 70, 5007 Bergen, Norway
e-mail: juergen.bader@bjerknes.uib.no

The purpose of this study is twofold. First, we want to isolate the impact of projected future modifications to the seasonal cycle of Arctic sea-ice cover on extratropical storminess. Second, we will scrutinize the seasonality of the weak winter response of the NAO. We show that the winter response is dominated by the March response. Only in March is an eddy forcing consistent with negative NAO events (Limpasuvan and Hartmann 2000) able to induce a much larger response. The importance of seasonality for the NAO response to sea-ice anomalies has not been demonstrated before.

2 Model and experiments

Two 31-year long experiments are performed with the atmospheric general circulation model ECHAM5 (Roeckner et al. 2003). The atmospheric model is run at T42 ($\approx 2.8^\circ \times 2.8^\circ$) horizontal resolution with 19 vertical levels. A present day integration is forced by the 1981–1999 Hadley Centre observations (Rayner et al. 2003) of the climatological seasonal cycle of sea surface temperatures (SSTs) and sea ice concentrations (SICs). The Arctic SIC field in the second experiment is changed to a projected climatological seasonal cycle, based on the 2081–2099 ECHAM5/MPI-OM IPCC SRESA1B scenario output of three ensemble members. The Arctic sea-ice thickness is fixed at 2m in both experiments. For the experiment with projected sea ice the sea surface temperatures in the northern hemisphere have been replaced with projected SSTs at grid points where sea ice has changed. Elsewhere the SSTs are the same as in the present day experiment. Results are averaged over the last 30 years and only the mean response (projected – present day) is presented here. Figure 1a shows the reduction in sea ice concentration in January between the two experiments. Except over Hudson Bay, this spatial pattern is very consistent throughout February and March. The sea-ice reduction in December covers a slightly larger area (not shown). The ECHAM5/MPI-OM IPCC SRESA1B output has been shown to have a stronger decline in sea ice concentration than the IPCC ensemble mean (Stroeve et al. 2007). Figure 1b and c show the seasonality of differences in latent and sensible heat fluxes between the two experiments. Positive values are indicative of increased ocean-to-atmosphere heat fluxes (projected minus present day) when sea-ice concentration is reduced. Only positive values are shown since the NAO response itself is associated with negative heat fluxes that is only indirectly linked to sea-ice anomalies. It is clear that the largest response in heat forcing is during the winter season (NDJFM), though the biggest sea-ice reduction is in September (not shown). Note the small difference in the spatial distribution of heat fluxes between January and

March shown in Fig. 1c. The main difference being slightly larger fluxes from the Labrador Sea and Hudson Bay in January.

3 Results

Figure 2a shows the winter mean DJF 500 hPa geopotential height response. A significant positive height anomaly can be seen throughout the Arctic with a maximum amplitude of 50m. Both the amplitude and spatial pattern are similar to the atmospheric response documented in Alexander et al. (2004). However, our focus here is not on the winter mean but rather to highlight the March response shown in Fig. 2b. The 500 hPa response during March has a maximum amplitude of 90m and projects strongly on the model-NAO. The NAO being defined as the first EOF of 500 hPa height anomalies (DJFM) in the North Atlantic sector (90°W – 40°E , 20°N – 90°N) in the present day integration. This is surprising as the change in surface energy fluxes are

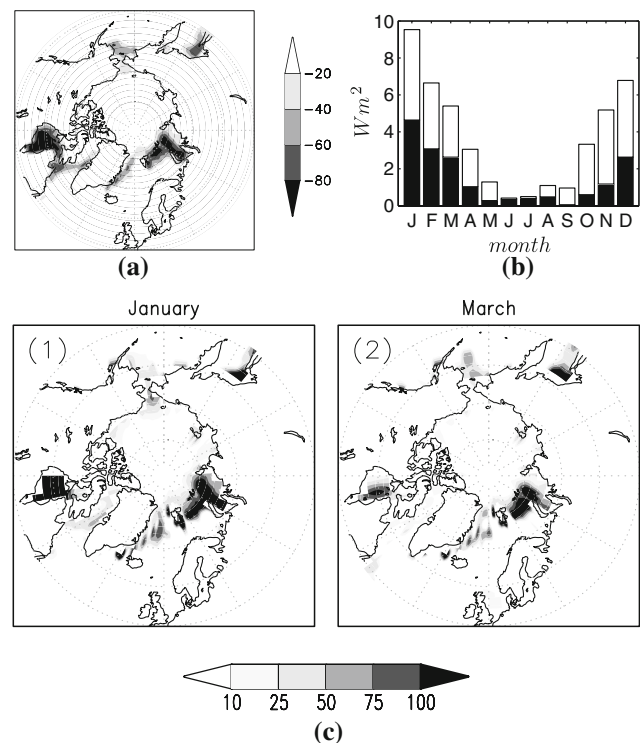


Fig. 1 **a** The projected reduction (%) in sea-ice concentration in January between ECHAM5/MPI-OM IPCC SRESA1B scenario for 2081–2099 and present day climatology (1981–1999). **b** The difference in sensible heat (black) and latent heat (white) input to the atmosphere from the ocean between the two experiments. The heat forcing is area-weighted and averaged over all sea-ice and water grid points between 55°N and 90°N . Units are in W m^{-2} . **c** Same as **b** but shown as spatial maps for January(1) and March(2) and without area weighted averaging. Only upward fluxes (ocean to atmosphere) are shown

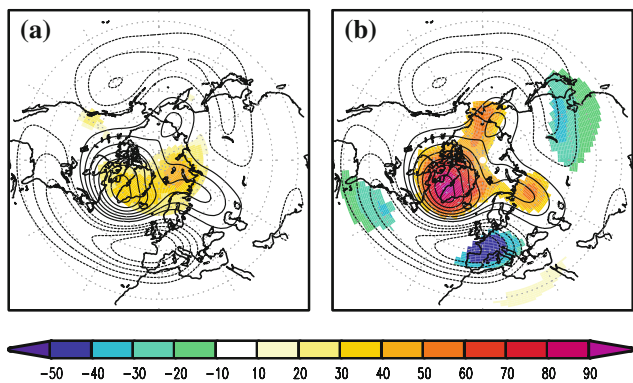


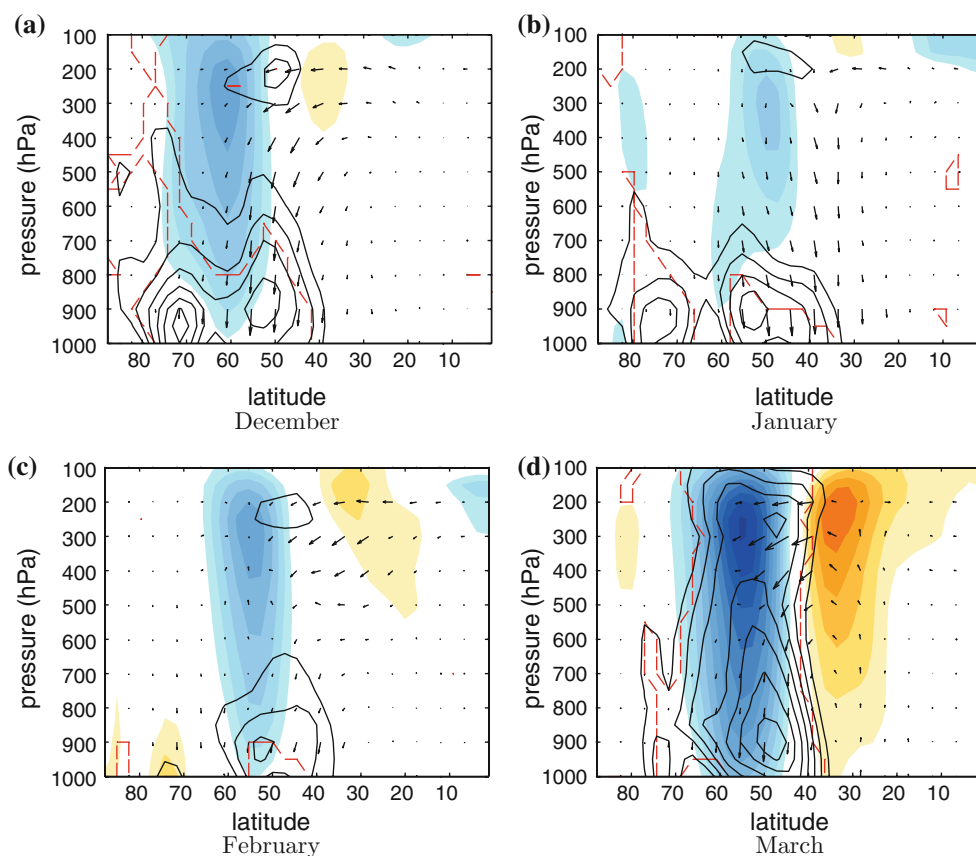
Fig. 2 **a** Color: The winter mean (DJF) response in 500 hPa geopotential height. Only areas statistically significant at the 5% level are colored. **b** Color: The March response in 500 hPa geopotential height. Superimposed contour lines in both figures: the negative phase of the first EOF in the Atlantic sector of winter 500 hPa geopotential height anomalies. Contour interval is 10m. *Solid lines* are positive anomalies and *dashed* are negative

smaller in March than in the other winter months (Fig. 1b). In April no significant response in 500 hPa geopotential height was found (not shown). In addition to the *t* test shown in Fig. 2 the statistical significance of the March response was assessed using a permutation test. 30 months were drawn randomly 10,000 times from the winter months

DJFM in both experiments. The mean 500 hPa geopotential height difference was each time calculated for the sample of months and projected onto the NAO pattern. These values were then compared with the threshold value of the March response projected on the NAO. This test yielded a *p* value of 0.02.

The seasonality of the response can also be seen in extratropical storminess. The chosen measure of storminess is the 2–8 day bandpass filtered poleward heat flux ($\overline{v't'}$) which is known to reflect baroclinic wave activity (Wallace et al. 1988). The heat flux is a low-level measure of the winter climatological storm track since it peaks in the model at about 800 hPa at 45°N. The zonal mean response is shown in Fig. 3. In December the storminess is clearly reduced with a peak of -1.4 K m s^{-1} close to 70°N. There is also a significant reduction at midlatitudes between 50 and 60N. The January response is similar but with smaller amplitude. The smallest response is found in February with a barely significant reduction at 52°N. However, the March response again clearly stands out. There is a much larger response at midlatitudes with a significant reduction throughout the depth of the troposphere. The March reduction can therefore also be seen using storminess indicators dominating at upper levels such as high-pass filtered eddy kinetic energy $\frac{1}{2}(\overline{v'^2 + u'^2})$. In the North

Fig. 3 Coloring: Zonal mean zonal wind response. Contour interval is 0.25 m/s. *Blue colours* are negative and *red* are positive. *Black contours*: Decrease in storminess defined as the mean 2–8 day bandpass filtered eddy heat flux ($\overline{v't'}$). Contour interval is 0.2 K m s^{-1} starting at a reduction of 0.4 K m s^{-1} . *Red dashed line* shows the statistical significance at the 5% level. The anomalous Eliassen–Palm flux vectors based on monthly mean data are superimposed on the plots. The vectors are scaled following Edmon et al. (1980) and the longest vector is $4.5 \times 10^{19} \text{ m}^3 \text{ s}^{-2}$. Convergence/divergence of the EP flux vectors implies easterly/westerly acceleration of the flow by the monthly eddy forcing



Atlantic, the March eddy kinetic energy reduction at 250 hPa exceeds 30% at the downstream end of the storm track (not shown).

Figure 3 also shows the response of the zonal mean zonal wind. It is only in March we find a response that closely resembles the dipole of NAO/NAM wind anomalies (i.e Limpasuvan and Hartmann 2000). However, in all the months (perhaps with the exception of January) the responses are largely equivalent barotropic suggesting that they are driven by changes in transient eddy fluxes. To investigate the way the transient eddies interact with the mean flow we adopt the quasi-geostrophic transformed Eulerian mean (TEM) framework of zonal momentum balance (Edmon et al. 1980):

$$\frac{\partial [u]}{\partial t} - f[v]^* - R = (r_0 \cos \phi)^{-1} \nabla \cdot F \tag{1}$$

$$F = \left\{ -r_0 \cos \phi [u'v'], fr_0 \cos \phi \frac{[v'\theta']}{\partial[\theta]/\partial p} \right\} \tag{2}$$

where brackets denote zonal mean values, u is zonal wind, v^* the residual meridional wind and F the Eliassen–Palm flux vector. The other notation follows Edmon et al. (1980). Transient eddies are defined as departures from monthly mean values. Figure 3 shows the response in EP-fluxes. Consistent with a decreasing poleward transient heat flux, there is less upward propagating wave activity in all the months although only weakly so in February. At upper levels there is less equatorward propagation of wave activity, in particular in December and March. The horizontal component of the EP-flux is proportional to the negative of the eddy momentum flux (see Eq. 2). At upper levels there is therefore anomalous divergence of eddy momentum flux and hence deceleration of the zonal mean zonal wind. The forcing from transient eddies thus act to maintain the mean response.

Since the March response is substantially larger than in the other months, we want to investigate whether it is driven by the same feedback from eddy forcing as for negative NAO events. It has been shown that monthly changes in the NAO/NAM index are driven by feedbacks from the forcing of both transient and quasi-stationary eddies (Limpasuvan and Hartmann 2000; Lorenz and Hartmann 2003). Quasi-stationary eddies are defined in Eq. 2 as departures from the zonal mean for a given month. The spatial pattern of the NAO is the same as shown in Fig. 2. Only the vertically averaged (700–100 hPa) forcing due to the eddy momentum flux divergence is considered and we will refer to it as the barotropic forcing.

Figure 4 shows the difference in barotropic forcing between the composite of negative NAO months (below -1 standard deviation) and climatology in the present day experiment (DJFM). It shows that monthly zonal wind anomalies associated with negative NAO events are driven by the divergence of both quasi-stationary and transient momentum fluxes at midlatitudes. The contribution from quasi-stationary eddies being somewhat more poleward at midlatitudes, while the divergence at 35°N is dominated by transient fluxes. This forcing is then compared to those of the projected experiment for each month. The response in barotropic forcing for March is shown in Fig. 4b (solid lines). The transient forcing can be seen to closely follow negative NAO events at both centers of the dipole. The quasi-stationary forcing is also similar to the NAO although it is more meridionally confined at midlatitudes. The response in December shown in Fig. 4a does not exhibit the same resemblance to the NAO forcing. At 50°N the quasi-stationary and transient forcing can be seen to even oppose each other. Neither January nor February resembles the barotropic forcing of the negative NAO phase (not shown). March is therefore the only month

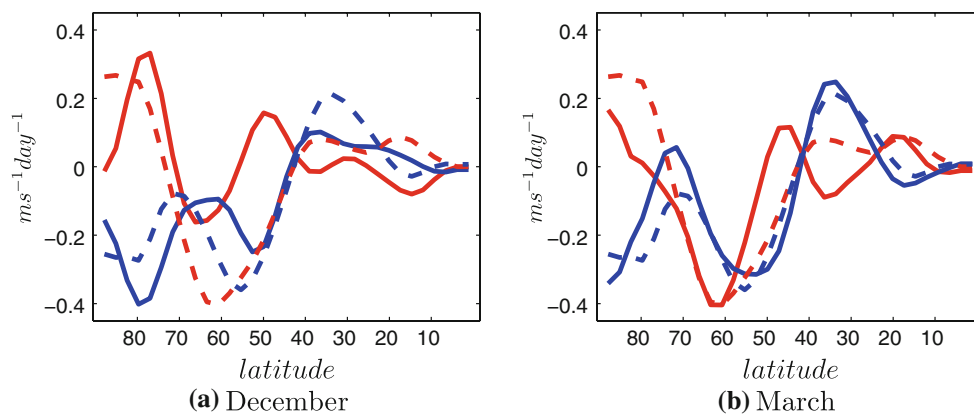


Fig. 4 Vertically averaged (700–100 hPa) forcing of the zonal mean zonal wind due to eddy momentum flux divergence. Units are in $\text{m s}^{-1} \text{day}^{-1}$. The solid lines are the response in forcing for **a** December and **b** March. Dashed lines are the difference in forcing between the

composite of negative NAO months below -1 standard deviation and climatology (multiplied by 0.7 for ease of comparison). Red lines show the difference in quasi-stationary wave forcing. Blue lines denote the difference in transient wave forcing

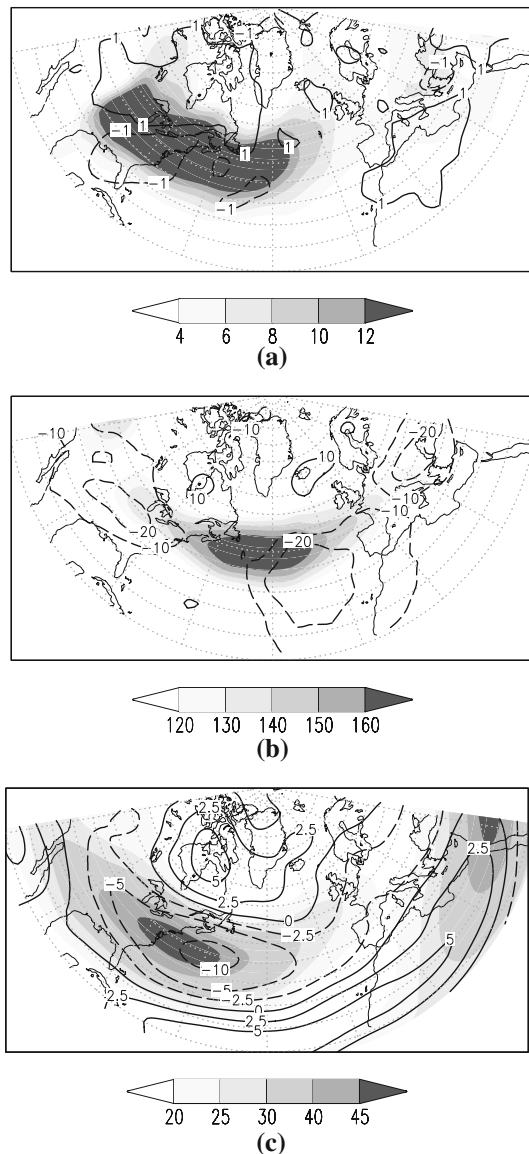


Fig. 5 **a** Shading: January climatological stormtracks (from present day run) defined as the mean 2–8 day bandpass filtered eddy heat flux ($\overline{v't'}$). Contours: March climatology relative to January. Units in K m s^{-1} . **b** Same as **a** but for 2–8 day bandpass filtered EKE at 250 hPa ($\frac{1}{2}(\overline{v'^2} + \overline{u'^2})$). Units in $\text{m}^2 \text{s}^{-2}$. **c** Same as **a** but for zonal wind at 250 hPa. Units in m s^{-1}

triggering the eddy forcing associated with negative NAO events.

Since there is little evidence that differences in ocean–atmosphere fluxes can account for the seasonality of the response, we turn to the seasonality of the circulation in the model. Figure 5 shows the simulated North Atlantic storm track and the mean zonal wind for January and March. The 2–8 bandpass filtered meridional heat flux at 850 hPa can be seen in Fig. 5a. The January climatology peaks at the entrance of the North Atlantic storm track and compares well with the NCEP reanalysis (Chang et al. 2002). The

March climatology is not significantly different. Figure 5b shows the 2–8 day bandpass filtered EKE at 250 hPa. Relative to January the March climatology is weaker at the entrance of the storm track and shifted slightly poleward at the downstream end. The seasonality is greater in the background flow represented with the mean zonal wind at 250 hPa (Fig. 5c). In March the core of the eddy-driven jet is reduced by over 10 m s^{-1} and the subtropical jet is slightly stronger relative to January. But the question still remains why it is easier to trigger the negative NAO phase under the weaker zonal jet regime in March. Not only the background flow in the North Atlantic might be important as the forcing of the NAO was shown to include a contribution from quasi-stationary waves.

Kushnir et al. (2002) argued in the context of forcing from SST anomalies that the effect is likely to be biggest in the transition seasons, fall and spring, when atmospheric internal variability is reduced while strong eddy–mean flow interaction is still active.

However, even though November has less internal variability it is not dominated by NAO variability like the winter months DJFM (not shown). This may help to explain why the response in November, with comparable ocean–atmosphere fluxes to March, is much smaller.

4 Summary and conclusion

The impact of a reduced Arctic sea ice cover on wintertime extratropical storminess has been investigated by forcing the AGCM ECHAM5 with the present (1981–1999) and projected (2081–2099) seasonal cycles of Arctic sea ice. Significant reductions in low-level storminess were found in December and January, both at midlatitudes and towards the Arctic. However, the magnitudes were generally small and mostly confined to latitudes close to where sea-ice was removed. In February the response was barely significant. The common theme for DJF is thus that the removal of sea-ice reduces storminess locally but not much at midlatitudes.

The response in March was qualitatively different from that in December–February, with a large reduction in midlatitude storminess. This response is strongly associated with the negative phase of the NAO. It was also shown that this was consistent with a forcing from transient and quasi-stationary eddies associated with negative NAO events. We are thus confident that the sea-ice anomalies indeed triggered an increase in negative NAO events in March and less so in the other winter months. We therefore envisage that any important large scale influence of sea-ice anomalies depend on their ability to trigger the negative phase of the NAO.

The mean winter (DJFM) response to sea-ice anomalies found in this study compares well with other studies. Both

Alexander et al. (2004) and Magnúsdóttir et al. (2004) document similar negative NAO responses although the responses in the latter study are larger presumably because they removed all sea-ice in areas of sea-ice reduction. However, the response is somewhat at odds with the transient study of Singarayer et al. (2006) who also investigated the possible impact of a declining Arctic sea-ice cover. They found a *reduction* in sea-level pressure over the wintertime Arctic which is inconsistent with a negative NAO response. One way to interpret this difference is by separating the total response into a direct and indirect component as done by Deser et al. (2004). The indirect response projects strongly on the NAO with the characteristic eddy-driven equivalent barotropic structure in the vertical from the surface to the troposphere. In contrast, the direct response is localized to the surface heat anomaly and exhibits a *baroclinic* structure with a surface trough and upper level ridge. Since an increase in negative NAO events presumably were not triggered in Singarayer et al. (2006), the response may have been dominated by the direct component and therefore showed a reduction in Arctic sea-level pressure.

How relevant is the storm track response to sea-ice anomalies in a climate change context? One can envisage several competing influences under climate change scenarios. Storm growth may for instance increase as a result of an increasing upper level equator to pole temperature gradient or as a result of enhanced latent heat release in a moister atmosphere (Held 1993). Associated with enhanced warming in the tropical upper troposphere, Yin (2005) found a consistent poleward shift and intensification of the zonal mean storm tracks in an ensemble of twenty-first century climate simulations. In the eastern North Atlantic Ulbrich et al. (2008) found in a multi-model ensemble an increase of 5–8% in baroclinic wave activity by the end of the twenty-first century. Using the *coupled* version of the model used here, the ECHAM5/MPI-OM, both Bengtsson et al. (2006) and Pinto et al. (2007) reported an increase in winter cyclone intensities in the eastern North Atlantic. Since we found a *reduction* in storm track activity, there is little to suggest that these storm track responses are dominated by sea-ice anomalies. This is not surprising as we find the mean DJF storm track response to be small. However, none of the studies mentioned above showed the response in late winter alone. Our study suggests that if there is an imprint of the forcing from sea-ice anomalies it is likely to be found in late winter.

One should be careful not to generalize too much based on a single AGCM and a single set of boundary forcing anomalies. That said, Magnúsdóttir et al. (2004), using a different model and boundary conditions, stated briefly that the largest atmospheric response to their anomalies in sea-ice extent were also found in March. However, the

seasonality of the response was not addressed in their study. The implication from this study is that the background state can result in qualitatively different atmospheric responses, as demonstrated previously by the response to changed midlatitude SSTs (i.e. Peng et al. 1997; Peng and Robinson 2001). Furthermore, Deser et al. (2007) showed that a transient response to sea-ice anomalies reaches an equilibrium in the winter season. Our results do not support the existence of such an equilibrium. It is therefore a need to investigate the role of the background state for the response to sea-ice anomalies. At this stage it is not clear why the NAO is much more sensitive in March. Further experiments and analysis are planned to investigate this issue.

Acknowledgments We thank Nils Gunnar Kvamstø, Gudrun Magnúsdóttir and Justin Wettstein for insightful discussions. We thank the Max-Planck-Institute for Meteorology for providing and supporting the ECHAM5 model. The UK Meteorological Office and Hadley Centre is acknowledged for providing the HadISST 1.1—global sea-ice coverage and SST—dataset. We acknowledge the modeling groups, the Program for Climate Model Diagnosis and Intercomparison (PCMDI) and the WCRP's Working Group on Coupled Modelling (WGCM) for their roles in making available the WCRP CMIP3 multi-model dataset. Support of this dataset is provided by the Office of Science, US Department of Energy. This work was supported by the COMPAS and NorClim projects funded by the research council of Norway. The model runs have been performed at the Norwegian Metacenter For Computational Science (NOTUR) in Trondheim.

References

- Alexander MA, Bhatt US, Walsh JE, Timlin MS, Miller JS, Scott JD (2004) The atmospheric response to realistic Arctic sea ice anomalies in an AGCM during winter. *J Clim* 17:890–905
- Bengtsson L, Hodges KI, Roeckner E (2006) Storm tracks and climate change. *J Clim* 19:3518–3543
- Chang EKM, Lee SY, Swanson KL (2002) Storm track dynamics. *J Clim* 15:2163–2183
- Deser C, Magnúsdóttir G, Saravanan R, Phillips A (2004) The effects of North Atlantic SST and sea ice anomalies on the winter circulation in CCM3. Part II: Direct and indirect components of the response. *J Clim* 17:877–889
- Deser C, Tomas RA, Peng SL (2007) The transient atmospheric circulation response to North Atlantic SST and sea ice anomalies. *J Clim* 20:4751–4767
- Edmon HJ, Hoskins BJ, McIntyre ME (1980) Eliassen-Palm cross-sections for the troposphere. *J Atmos Sci* 37:2600–2616
- Eisenman I, Untersteiner N, Wettlaufer JS (2007) On the reliability of simulated Arctic sea ice in global climate models. *Geophys Res Lett* 34:L10501
- Held IM (1993) Large-scale dynamics and global warming. *Bull Am Meteorol Soc* 74:228–241
- Kushnir Y, Robinson WA, Blade I, Hall NMJ, Peng S, Sutton R (2002) Atmospheric GCM response to extratropical SST anomalies: synthesis and evaluation. *J Clim* 15:2233–2256
- Kvamstø NG, Skeie P, Stephenson DB (2004) Impact of Labrador sea-ice extent on the North Atlantic Oscillation. *Int J Climatol* 24:603–612

- Limpasuvan V, Hartmann DL (2000) Wave-maintained annular modes of climate variability. *J Clim* 13:4414–4429
- Lorenz DJ, Hartmann DL (2003) Eddy-zonal flow feedback in the Northern Hemisphere winter. *J Clim* 16:1212–1227
- Magnusdottir G, Deser C, Saravanan R (2004) The effects of North Atlantic SST and sea ice anomalies on the winter circulation in CCM3. Part I: Main features and storm track characteristics of the response. *J Clim* 17:857–876
- Peng SL, Robinson WA (2001) Relationships between atmospheric internal variability and the responses to an extratropical SST anomaly. *J Clim* 14:2943–2959
- Peng SL, Robinson WA, Hoerling MP (1997) The modeled atmospheric response to midlatitude SST anomalies and its dependence on background circulation states. *J Clim* 10:971–987
- Pinto JG, Ulbrich U, Leckebusch GC, Spanghel T, Reyers M, Zacharias S (2007) Changes in storm track and cyclone activity in three SRES ensemble experiments with the ECHAM5/MPI-OM1 GCM. *Clim Dyn* 29:195–210
- Rayner NA, Parker DE, Horton EB, Folland CK, Alexander LV, Rowell DP, Kent EC, Kaplan A (2003) Global analyses of sea surface temperature, sea ice, and night marine air temperature since the late nineteenth century. *J Geophys Res Atmos* 108:4407
- Singarayer JS, Bamber JL, Valdes PJ (2006) Twenty-first-century climate impacts from a declining Arctic sea ice cover. *J Clim* 19:1109–1125
- Stroeve J, Holland MM, Meier W, Scambos T, Serreze M (2007) Arctic sea ice decline: faster than forecast. *Geophys Res Lett* 34:L09501
- Ulbrich U, Pinto JG, Kupfer H, Leckebusch GC, Spanghel T, Reyers M (2008) Changing Northern Hemisphere storm tracks in an ensemble of IPCC climate change simulations. *J Clim* 21:1669–1679
- Wallace JM, Lim GH, Blackmon ML (1988) On the relationship between cyclone tracks, anticyclone tracks and baroclinic wave guides. *J Atmos Sci* 45:439–462
- Yin JH (2005) A consistent poleward shift of the storm tracks in simulations of 21st century climate. *Geophys Res Lett* 32:L18701
- Zhang XD, Walsh JE (2006) Toward a seasonally ice-covered Arctic Ocean: scenarios from the IPCC AR4 model simulations. *J Clim* 19:1730–1747